

# Oxytocin and Vasopressin Receptors in the Pouched Rat

Samanta Arenas<sup>a</sup>, Angela R. Freeman<sup>a</sup>, Bhupinder Singh<sup>b</sup>, Alexander G. Ophir<sup>\*,a</sup>

<sup>a</sup>Cornell University, Department of Psychology, Ithaca, NY, 14853

<sup>b</sup>Cornell University, Department of Veterinary Medicine, Ithaca, NY, 14853

## Abstract

This is the abstract. It consists of two paragraphs.

## Introduction

The neuropeptides oxytocin (OT) and vasopressin (AVP) modulate a variety of social behaviors including parental care, affiliation, and aggression, among other behaviors (Caldwell and Albers, 2015). These peptides act centrally through their associated receptors, the oxytocin (OTR) and vasopressin 1a and 1b (V1aR and V1bR) receptors. The nonapeptide system is well-conserved, evidenced by the presence of vasopressin or oxytocin or their homologues in mammals, birds, fish, snails, annelid worms and some insects (Donaldson and Young, 2008). Despite the conservation of the OT-AVP system, differences in the relative density and distribution of the OTR and V1aR exist between closely related species (e.g. Beery et al., 2008; Campbell et al., 2009; Insel et al., 1994; Kalamantios et al., 2010). These differences are thought to support species-specific ecology and mating tactic (Olazábal and Sandberg, 2020), and variation within a single species further supports this hypothesis (Barrett et al., 2013; Ophir et al., 2012, 2008; Zheng et al., 2013).

In addition to between- and within-species variation in the distribution and relative density of these receptors, several species exhibit sex differences in receptor density (Beery et al., 2008; Campbell et al., 2009; Dubois-Dauphin et al., 1991; Dumais et al., 2013; Dumais and Veenema, 2016; Insel et al., 1991; Smeltzer et al., 2006; Smith et al., 2017). These differences between the sexes are region-specific, and thought to support sex-specific behaviors (Dumais and Veenema, 2016). In other species, and other studies, however, there are no reported sex-differences in receptor distribution in OTR or V1aR in the brain (Freeman et al., 2019; Insel et al., 1994; Lim et al., 2004). Whether sex differences are reported are dependent on whether both sexes were studied, and whether areas that are sexually dimorphic with respect to receptor binding were measured. Furthermore, it is sometimes assumed that differences in density are biologically meaningful, or support functional differences, however, these assumptions are rarely tested directly. Indeed, in addition to differences in receptor distribution and density, which are thought to underlie sensitivity to nonapeptides, differences in release, innervation, and connectivity can all lead to altered function in the OT-AVP system. Thus, receptor distribution and density is an important part of the nonapeptide system, but other differences in this system can modulate function and behavior.

In order to understand the evolutionary A recent metaanalysis of the distribution and relative density of OTR and V1aR in rodents demonstrated that OTR and V1aR have had different selective pressures leading to variation

32 among species (Freeman et al., 2020). V1aR distribution and density tends to be highly conserved within genera,  
33 whereas OTR tends to be labile (Freeman et al., 2020). Additionally, certain brain regions tend to have correlated  
34 binding of OTR (BNST, CeA), while others tend to be highly variable across species (VMH, MeA). V1aR, however,  
35 shows that binding in the LS and VPall are correlated in rodents, and tend to covary

36 For example, nonmonogamous voles (e.g. Montane (*Microtus montanus*) and Meadow voles (*Microtus pennsylvanicus*)) have relatively denser V1aR binding in the lateral septum compared to closely-related socially monogamous voles (e.g. Prairie (*Microtus Ochrogaster*) and Pine voles (*Microtus pinetorum*)) (Insel et al., 1994). Furthermore, V1aR in the lateral septum is positively associated with high levels of social investigation in male prairie voles, while this behavior is negatively associated with OTR in the same region [Ophir2009a]. OTR signalling in prairie voles, however, supports partner preference [Johnson2016], and higher densities in the nucleus accumbens is associated with a monogamous mating tactic [Ophir2012]. Outside of the *Microtine* voles, OTR and V1aR distributions have been compared in tuco-tucos, where Beery et al. reported denser OTR binding in the lateral septum in *Ctenomys haigi* compared to *Ctenomys sociabilis*, even though *C. Haigi* is solitary, and *C. sociabilis* is colonial [Beery2008]. In singing mice (*Scotinomys spp.*), two vocal and social species that differ in density and space use patterns both had

- 47 • What do we know about the distribution and relative densities of receptors (i.e. what can it tell  
48 us, what's been done on behavior?)

49 -How might life history differences play into patterning of central distribution of these receptors?

50 -What tends to be conserved?

51 -How does comparative analysis help? (Kelly and Ophir, 2015)

52 -Why did we do this study? What were we examining?

53 -We wanted to describe the presence and relative density of OTR and V1aR in pouched rat brains in  
54 males and females, to see if there were differences in presence and density between sexes

55 -We wanted to explore how the patterning of these receptors might differ from other rodents and see if  
56 it further supports the ideas found in the recent metaanalysis (Freeman et al., 2020)(see where pouched  
57 rats fall in this framework)

## 58 Methods

59 All work with animals was approved under the U.S. Army Medical Research and Materiel Command (USAM-RMC) Animal Care and Use Review Office (ACURO) and the Cornell Institutional Animal Care and Use Committee (IACUC 2014-0043). Tissues were collected from wild-caught animals from Morogoro, Tanzania (6°49'49"S,

62 37°40'14"E). Prior to collection, animals were housed individually in standard rabbit enclosures and maintained on  
63 a 12:12 h light:dark light cycle, at 21°C and 45% humidity. Males and females were kept in separate rooms. Animals  
64 were fed a standard rodent diet supplemented with dog kibble and fresh fruit and vegetable treats. Chewing bones,  
65 a metal 'stovepipe' hutch, and dog puzzle toys were given as behavioral enrichment. Newspaper was given for  
66 nesting material.

67 Animals were euthanized via CO<sub>2</sub> inhalation and brains were swiftly removed and frozen using liquid nitrogen  
68 or powdered dry ice and stored at -80°C prior to sectioning. Ten male and ten female brains were used for this  
69 study. Brains were blocked coronally by removing the cerebellum, then split sagittally next to the midline into two  
70 hemispheres, and one hemisphere (preferably the left if unblemished) was coronally sectioned at 20µm thick using a  
71 Leica cryostat (CM1950, Leica Biosystems, Nussloch, Germany) set at -20°C. Due to the large size of the pouched  
72 rat brains, we mounted every 3rd section and kept 6 serial sets. Sections were collected from the olfactory bulbs  
73 to the start of the cerebellum, and mounted on Superfrost Plus Microscope sides (Fisher Scientific, Pittsburg, PA  
74 USA). Microscope slides were stored at -80°C until the autoradiography procedure.

75 On two of the sets of slides, we used <sup>125</sup>I radioligands to label oxytocin receptor (ornithine vasopressin analog,  
76 <sup>125</sup>I-OVTA); NEX 254, PerkinElmer; Waltham, MA) or vasopressin 1a receptor (vasopressin (Linear), V-1A antag-  
77 onist (Phenylacetyl1, 0-Me-D-Tyr2 [ <sup>125</sup>I-Arg6 ]-); NEX 310, PerkinElmer), as described by Ophir and colleagues  
78 (Ophir et al., 2013). Following processing and air-drying, we exposed radiolabeled tissue to film (Kodak Carestream  
79 Biomax MS) for 6 days for OTR and 2 days for V1aR to account for differing degrees of decay at the time of use.  
80 In each film cassette, we included two <sup>125</sup>I microscales (American Radiolabeled Chemicals; St Louis, MO), to allow  
81 for the conversion of optical density to receptor density. We inferred that receptor density relates to optical density  
82 of exposed film to use optical measurements as a proxy for receptor density. We digitized films on a Microtek  
83 ArtixScan M1 (Microtek, Santa Fe Springs, CA) and measured optical densities using NIH ImageJ Software. We  
84 calculated receptor density by first converting optical density to disintegrations per minute (dpm) adjusted for tissue  
85 equivalence (TE; for 1 mg in the rat brain), by fitting curves generated by radiographic standards and extrapolating  
86 based on these standard curves for each film.

87 Three sequential sections were measured for density by encircling the regions of interest using NIH ImageJ  
88 software. The software program calculated mean optical density values and area for regions of interest (ROI). We  
89 measured background labelling by measuring optical density from an area of cortex in the same section for each  
90 region of interest. To correctly identify ROI, we Nissl-stained a third set of tissue to use as a reference, in conjunction  
91 with anatomical landmarks identified using a Rat brain atlas. The three measurements for each individual's ROIs  
92 and background were averaged separately, and background was subtracted from the ROI to yield receptor density.  
93 These final measurements were used for all statistical tests, tables, and figures.

94 OTR density was measured in the olfactory bulb (OB), anterior olfactory nucleus (AON), prefrontal cortex  
95 (PFC), piriform cortex (Pir), nucleus accumbens (NAcc), lateral septum (LS), endopiriform (Den), claustrum

96 (VCL), lateral bed nucleus of the stria terminalis (BSTl), medial bed nucleus of the stria terminalis (BSTm),  
97 ventral bed nucleus of the stria terminalis (BSTv), ventral pallidum (VPall), medial preoptic area (MPOA), ante-  
98 rior hypothalamus (AH), paraventricular thalamus (PVT), suprachiasmatic nucleus (SCN), paraventricular nucleus  
99 (PVN), magnocellular hypothalamic nucleus (MCPO), medial habenula (MHb), central amygdala (CeA), medial  
100 amygdala (MeA), basolateral amygdala (BLA), ventromedial hypothalamus (VMH), zona incerta (ZIR), lateral  
101 hypothalamus (PrFLH), hippocampal CA1, hippocampal CA2, hippocampal CA3, dentate gyrus (DG), premam-  
102 milary ventral nucleus (PMV), ventral tegmental area (VTA), periaqueductal gray (PAG), medial geniculate (MG),  
103 superior colliculus (SuG), and the ventral CA3. V1aR was measured in the same regions except for the MCPO and  
104 the MHb.

105 To calculate ‘relative binding’ on a 4-point scale, we used the following definitions: mean OTR < 35 dpm/mg:  
106 absent/-, 35 to 490: present/+, 490 to 945: moderate/++, 945 to 1400: dense/+++; mean V1aR < 100 dpm/mg:  
107 absent/-, 100-1367: present/+, 1367 to 2634: moderate/++, 2634 to 3800: dense/+++. To compare receptor  
108 densities between sexes, we conducted t-tests for each region. We used a bonferroni correction to adjust for multiple  
109 comparisons. Test statistics were considered significant when  $p < 0.05$ .

110 We used the framework from Freeman et al. (2020) to compare overall binding patterns in the pouched rat to  
111 those in other rodents (Freeman et al., 2020). This framework uses overall OTR and V1aR binding patterns to  
112 examine similarities among species, genera, and family groups. Briefly, relative binding patterns within a species  
113 are converted to a 4-point scale, using wording and data from previously published studies. These data are then  
114 used in a principal components analysis, and species are plotted along the PC1 and PC2 components, with vectors  
115 in the plot serving as weights of each variable, and the direction indicating loading on PC1 and PC2.

116 We mapped pouched rat relative binding data onto this plot based on this framework and the data presented  
117 in this study. In addition to superimposing the pouched rat onto the PCA biplot, we conducted a comparative  
118 permutational anova (Adonis function) to examine whether genus or family groups predicted similarities among  
119 species’ relative binding patterns using the previously published data and the data from this paper. All analyses  
120 were conducted in R 4.0.2, with the vegan package for the ‘adonis’ function, and stats package for t tests and  
121 principal components analysis (R Development Core Team, 2016). PCA biplots were made using the ggbioptplot  
122 function in the ggbioptplot package with some aesthetic changes.

## 123 Results

124 After comparing male and female densities in the measured regions, most regions showed no differences between  
125 sexes. The superior colliculus had higher densities of OTR in females compared to males (Table 1, Female mean:  
126 199.35, Male mean 51.46,  $t_{(13.58)} = 2.79$ ,  $p = 0.01$ ), however, this was no longer significant after corrections for  
127 multiple comparisons (adjusted  $\alpha = 0.001$ ).

Table 1: OTR densities by region and sex

Region	Sex	Density mean $\pm$ SE (dpm/mg)	N
Olfactory Bulb	F	126.27 $\pm$ 39.56	9
Olfactory Bulb	M	142.74 $\pm$ 39.34	9
Accessory Olfactory Nucleus	F	186.38 $\pm$ 40.35	9
Accessory Olfactory Nucleus	M	144.1 $\pm$ 30.98	9
mPFC	F	117.96 $\pm$ 36.91	9
mPFC	M	94.51 $\pm$ 32.08	9
Infralimbic Cortex	F	138.22 $\pm$ 43.25	9
Infralimbic Cortex	M	72.54 $\pm$ 20.32	9
Nac Core	F	46.18 $\pm$ 14.48	9
Nac Core	M	37.34 $\pm$ 12.45	9
Nac Shell	F	81.44 $\pm$ 17.96	9
Nac Shell	M	51.75 $\pm$ 13.37	9
Caudate Putamen	F	30.8 $\pm$ 13.39	9
Caudate Putamen	M	23.93 $\pm$ 8.42	9
Piriform Cortex	F	222.05 $\pm$ 39.71	9
Piriform Cortex	M	192.1 $\pm$ 35.8	9
Lateral Septum I	F	55.24 $\pm$ 12.25	11
Lateral Septum I	M	57.94 $\pm$ 13.57	9
Lateral Septum D	F	48.7 $\pm$ 7.59	11
Lateral Septum D	M	56.22 $\pm$ 12.33	9
Lateral Septum V	F	71.16 $\pm$ 16.63	11
Lateral Septum V	M	103.53 $\pm$ 35.63	9
Endopiriform Cortex	F	147.07 $\pm$ 22.53	10
Endopiriform Cortex	M	111.82 $\pm$ 19.71	9
Clastrum	F	192.58 $\pm$ 47.69	10
Clastrum	M	193.17 $\pm$ 28.09	9
BSTm	F	585.91 $\pm$ 117.64	10
BSTm	M	532.58 $\pm$ 91.23	9
BSTi	F	687.03 $\pm$ 132.48	10
BSTi	M	425.66 $\pm$ 79.05	9
BSTv	F	101.57 $\pm$ 21.35	10

Region	Sex	Density mean $\pm$ SE (dpm/mg)	N
BSTv	M	92.97 $\pm$ 28.24	9
Ventral Pallidum	F	107.32 $\pm$ 15.18	10
Ventral Pallidum	M	78.04 $\pm$ 23.15	9
MPOA	F	95.77 $\pm$ 19.61	10
MPOA	M	88.22 $\pm$ 17.61	9
Anterior Hypothalamus	F	90.27 $\pm$ 24.22	10
Anterior Hypothalamus	M	74.19 $\pm$ 17.25	7
PVT	F	50.91 $\pm$ 16.77	10
PVT	M	64.52 $\pm$ 27.91	7
SCN	F	80.48 $\pm$ 23.44	10
SCN	M	125.57 $\pm$ 45.86	7
PVN	F	14.44 $\pm$ 16.18	9
PVN	M	93.85 $\pm$ 41.77	7
Medial Hypothalamic Nucleus	F	118.68 $\pm$ 37.66	9
Medial Hypothalamic Nucleus	M	122.42 $\pm$ 33.6	7
Medial Habenula	F	545.93 $\pm$ 121.71	10
Medial Habenula	M	648.41 $\pm$ 97.33	9
Central Amygdala	F	695.23 $\pm$ 144.28	9
Central Amygdala	M	734.04 $\pm$ 92.77	9
Medial Amygdala	F	328.84 $\pm$ 51.14	9
Medial Amygdala	M	380.99 $\pm$ 82.29	9
Basolateral Amygdala	F	627.27 $\pm$ 120.17	9
Basolateral Amygdala	M	712.9 $\pm$ 155.24	9
VMH	F	1242.79 $\pm$ 245.41	9
VMH	M	1224.42 $\pm$ 165.26	9
Zona Incerta	F	408.51 $\pm$ 67.31	10
Zona Incerta	M	415.41 $\pm$ 58.07	9
Lateral Hypothalamus	F	176.03 $\pm$ 32.85	10
Lateral Hypothalamus	M	171.5 $\pm$ 41.95	9
CA1	F	121.81 $\pm$ 25.41	11
CA1	M	107.19 $\pm$ 15.49	9
CA2	F	106.13 $\pm$ 11.57	11

Region	Sex	Density mean $\pm$ SE (dpm/mg)	N
CA2	M	127.54 $\pm$ 25.3	9
CA3	F	39.48 $\pm$ 10.47	11
CA3	M	45.77 $\pm$ 10.29	9
Premammillary Nucleus	F	535.99 $\pm$ 110.84	10
Premammillary Nucleus	M	499.3 $\pm$ 106.84	9
VTA	F	523.97 $\pm$ 74.13	9
VTA	M	628.2 $\pm$ 174.1	9
PAG	F	191.21 $\pm$ 35.76	10
PAG	M	106.35 $\pm$ 28.22	7
Superior Colliculus	F	199.35 $\pm$ 46.21	10
Superior Colliculus	M	51.46 $\pm$ 26.08	7

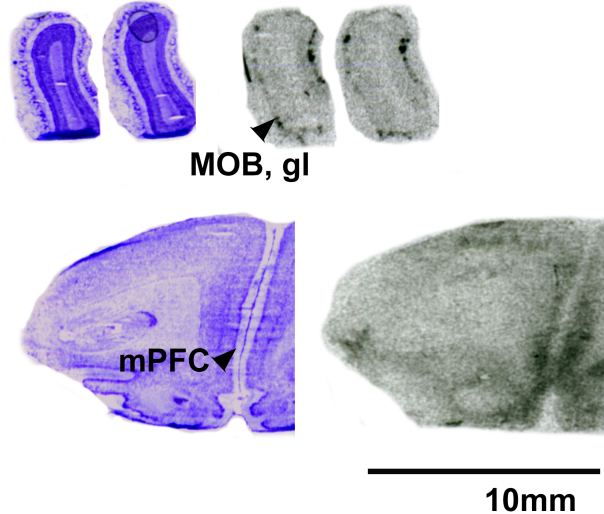


Figure 1: OTR in the forebrain of the pouched rat. Images on left are Nissl stain, associated autoradiograms on right show OTR density. MOB, gl = Main olfactory bulb, glomerular layer, mPFC = medial prefrontal cortex.

<sup>128</sup> Pouched rats had very dense OTR binding in the VMH, with moderate binding in the BNST, CeA and VTA.  
<sup>129</sup> There was only a low level of binding in the OB and mPFC (Table 2, Figure 1). Extremely low levels of OTR  
<sup>130</sup> binding were observed in NAcc, LS, PVN, and thalamus (Figures 2-4).

Table 2: OTR relative densities in select regions

Region	Relative.Binding
Olfactory Bulb	+
Nucleus Accumbens	+
mPFC	+
Ventral Pallidum	-
Lateral Septum	+
BST	++
CeA	++
MeA	+
Hippocampus	+
VMH	+++
VTA	++

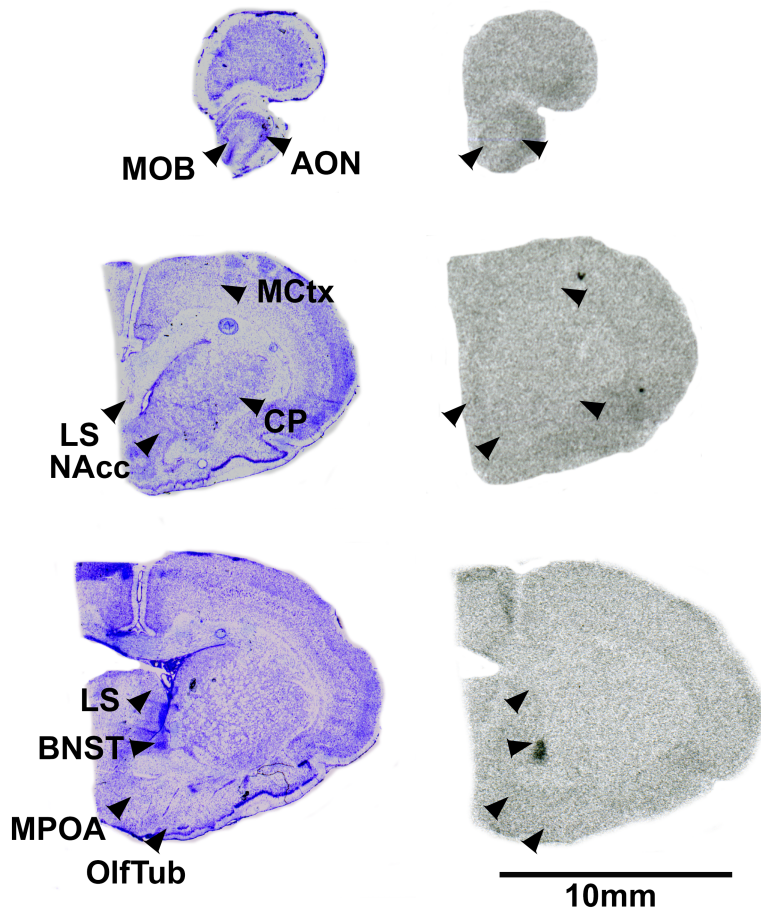


Figure 2: OTR in the forebrain of the pouched rat. Images on left are Nissl stain, associated autoradiograms on right show OTR density. MOB = Main olfactory bulb, AON = accessory olfactory nucleus, LS = lateral septum, CP = caudate putamen, MCtx = motor cortex, NAcc = nucleus accumbens, MPOA = medial preoptic area, OlfTub = olfactory tubercle.

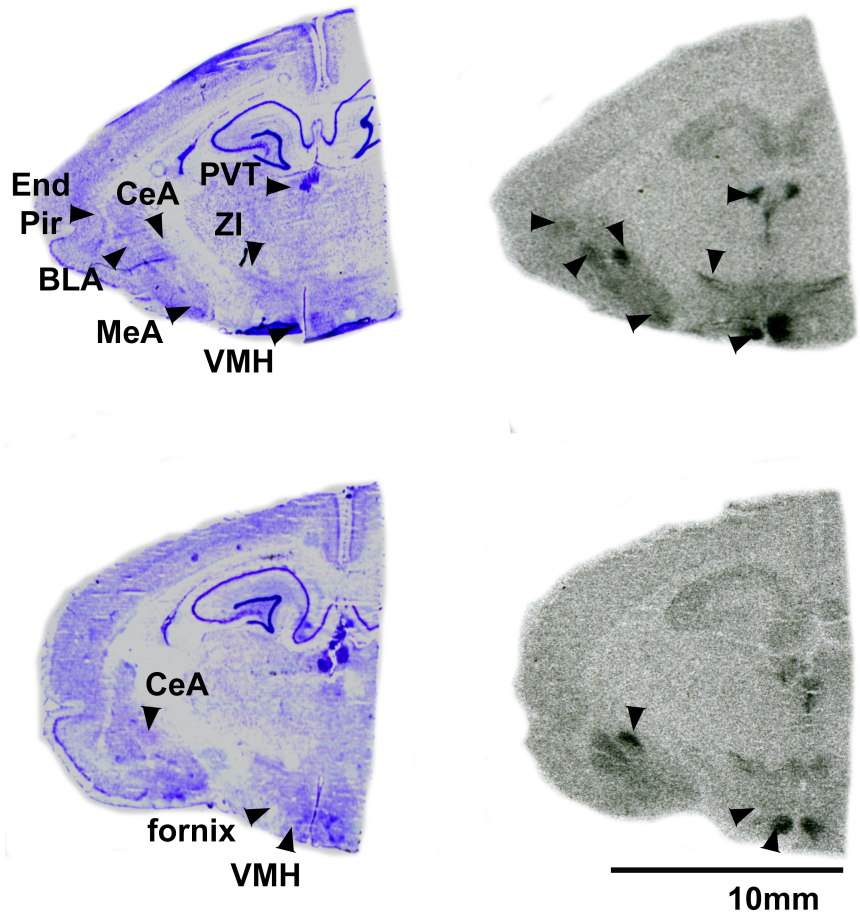


Figure 3: OTR in the forebrain of the pouched rat. Images on left are Nissl stain, associated autoradiograms on right show OTR density. End Pir = Endopiriform Nucleus, BLA = Basolateral Amygdala, MeA = Medial Amygdala, CeA = Central Amygdala, VMH = Ventromedial Hypothalamic Nucleus, ZI = Zona Incerta, PVT = Periventricular Thalamic Nucleus.

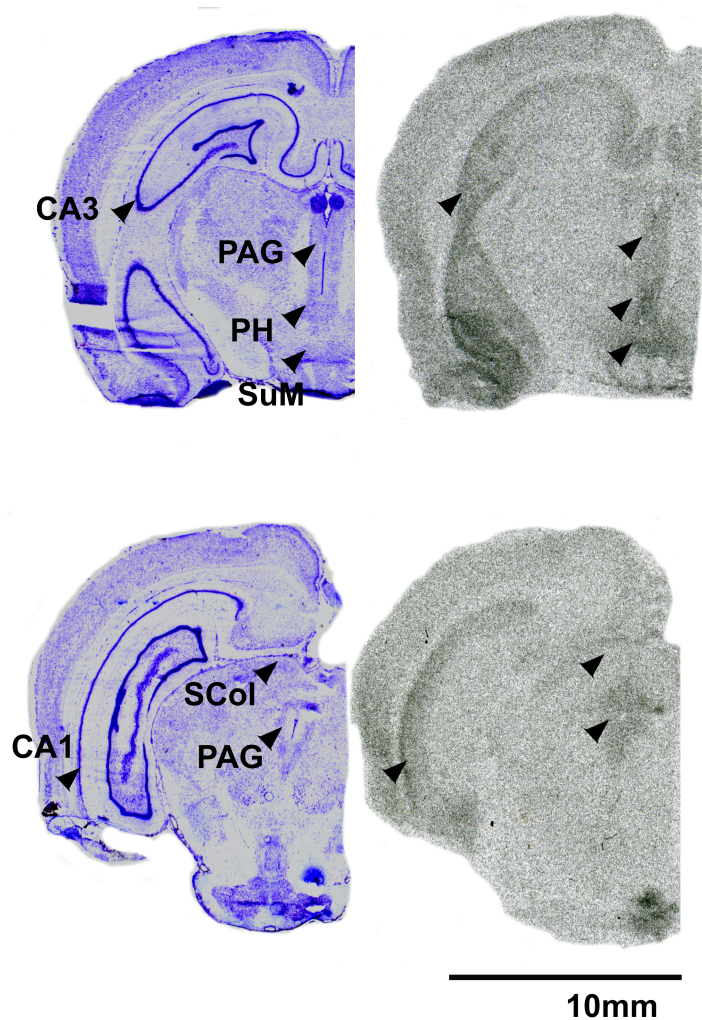


Figure 4: OTR in the forebrain of the pouched rat. Images on left are Nissl stain, associated autoradiograms on right show OTR density. CA3 = CA3 region of the Hippocampus, CA1 = CA1 region of the Hippocampus, PAG = Periacqueductal Grey, PH = Posterior Hypothalamic Nucleus, SCol = Superior Colliculus, SuM = Supramammillary Nucleus

Table 3: V1aR densities by region and sex

Region	Sex	Density mean $\pm$ SE (dpm/mg)	N
Olfactory Bulb	F	1456.47 $\pm$ 244.89	9
Olfactory Bulb	M	1841.49 $\pm$ 278.59	8
Accessory Olfactory Nucleus	F	1287.3 $\pm$ 173.38	9
Accessory Olfactory Nucleus	M	1596.88 $\pm$ 235.76	8
mPFC	F	588.16 $\pm$ 73.53	11
mPFC	M	604.41 $\pm$ 115.62	9
Infralimbic Cortex	F	388.15 $\pm$ 52.78	11
Infralimbic Cortex	M	426.68 $\pm$ 111.74	9
Nac Core	F	1319.1 $\pm$ 113.88	11
Nac Core	M	1748.56 $\pm$ 266.36	8
Nac Shell	F	1389.26 $\pm$ 169.07	11
Nac Shell	M	1687.58 $\pm$ 362.54	9
Caudate Putamen	F	1725.67 $\pm$ 148.69	11
Caudate Putamen	M	2329.94 $\pm$ 322	9
Piriform Cortex	F	604.16 $\pm$ 87.76	11
Piriform Cortex	M	649.05 $\pm$ 144.85	9
Lateral Septum I	F	3602.8 $\pm$ 355.47	11
Lateral Septum I	M	2885 $\pm$ 369.04	9
Lateral Septum D	F	3451.24 $\pm$ 276.7	11
Lateral Septum D	M	3613.44 $\pm$ 207.77	9
Lateral Septrum V	F	2395.85 $\pm$ 311.31	11
Lateral Septrum V	M	2351.65 $\pm$ 325.22	9
Endopiriform Cortex	F	296.6 $\pm$ 58.56	11
Endopiriform Cortex	M	260.42 $\pm$ 57.86	9
Clastrum	F	446.08 $\pm$ 74.68	11
Clastrum	M	334.95 $\pm$ 58.2	9
BSTm	F	1552.05 $\pm$ 161.04	11
BSTm	M	1452.1 $\pm$ 229.77	9
BSTi	F	1297.66 $\pm$ 80.59	11
BSTi	M	1056.38 $\pm$ 188.24	9
BSTv	F	885.07 $\pm$ 108.44	11

Region	Sex	Density mean $\pm$ SE (dpm/mg)	N
BSTv	M	835.57 $\pm$ 116.42	9
Ventral Pallidum	F	616.94 $\pm$ 104.42	11
Ventral Pallidum	M	470.4 $\pm$ 142.24	9
MPOA	F	626.46 $\pm$ 84.5	11
MPOA	M	522.26 $\pm$ 75.01	9
Anterior Hypothalamus	F	364.98 $\pm$ 97.49	9
Anterior Hypothalamus	M	601.09 $\pm$ 288.18	8
PVT	F	63.75 $\pm$ 58.22	9
PVT	M	245.11 $\pm$ 131.63	8
SCN	F	207.91 $\pm$ 109.3	9
SCN	M	85.55 $\pm$ 71.97	8
PVN	F	514.58 $\pm$ 146.84	8
PVN	M	520.91 $\pm$ 161.33	7
Central Amygdala	F	1710.61 $\pm$ 186.92	10
Central Amygdala	M	1439.79 $\pm$ 188.75	9
Medial Amygdala	F	841.82 $\pm$ 76.12	10
Medial Amygdala	M	928.64 $\pm$ 160.08	9
Basolateral Amygdala	F	120.35 $\pm$ 66.19	10
Basolateral Amygdala	M	139.62 $\pm$ 74.36	9
VMH	F	390.55 $\pm$ 130.5	10
VMH	M	576.42 $\pm$ 141.68	9
Zona Incerta	F	705.31 $\pm$ 78.81	10
Zona Incerta	M	738.07 $\pm$ 94.39	9
Lateral Hypothalamus	F	745.93 $\pm$ 91.88	10
Lateral Hypothalamus	M	915.03 $\pm$ 143.4	9
CA2	F	119.25 $\pm$ 56.35	11
CA2	M	63.4 $\pm$ 81.27	9
Dentate Gyrus	F	281.61 $\pm$ 107.99	11
Dentate Gyrus	M	347.83 $\pm$ 172.25	9
Premammillary Nucleus	F	1458.58 $\pm$ 333.09	11
Premammillary Nucleus	M	2206.81 $\pm$ 616.26	9
VTA	F	1132.57 $\pm$ 186.43	11

Region	Sex	Density mean $\pm$ SE (dpm/mg)	N
VTA	M	1278.42 $\pm$ 203.04	9
PAG	F	734.99 $\pm$ 97.71	11
PAG	M	947.68 $\pm$ 293.67	7
Medial Geniculate	F	93.87 $\pm$ 50.87	11
Medial Geniculate	M	147.82 $\pm$ 117.32	7
Superior Colliculus	F	819.1 $\pm$ 146.2	11
Superior Colliculus	M	744.4 $\pm$ 229.16	7
Ventral CA3	F	67.1 $\pm$ 78.53	5
Ventral CA3	M	119.62 $\pm$ 148.52	2

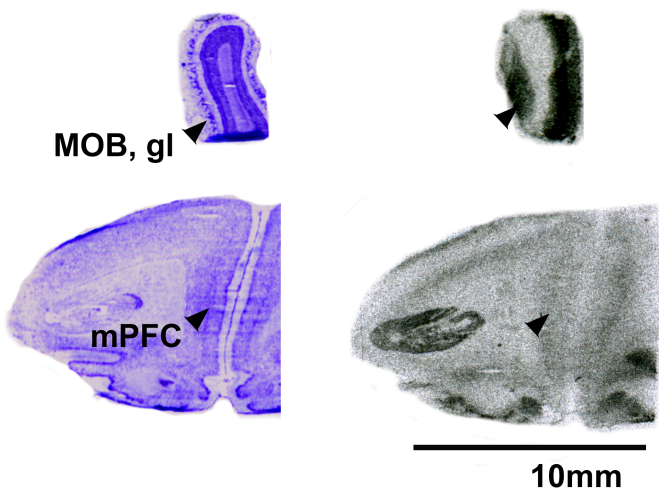


Figure 5: V1aR in the forebrain of the pouched rat. Images on left are Nissl stain, associated autoradiograms on right show V1aR density. MOB, gl = Main olfactory bulb, glomerular layer, mPFC = medial prefrontal cortex.

131 After comparing male and female densities of V1aR in the measured regions, we detected no significant differences  
 132 between sexes (Table 3).

133 Pouched rats had relatively very dense V1aR binding in the LS (Figure 6), and moderately dense levels of V1aR  
 134 binding in the Olfactory Bulbs, BST, NAcc, Amygdalar and Hypothalamic Nuclei (Figures 5-10). Binding in the  
 135 Hippocampus was generally absent except for some moderate V1aR binding in the most ventral regions (Figure  
 136 10).

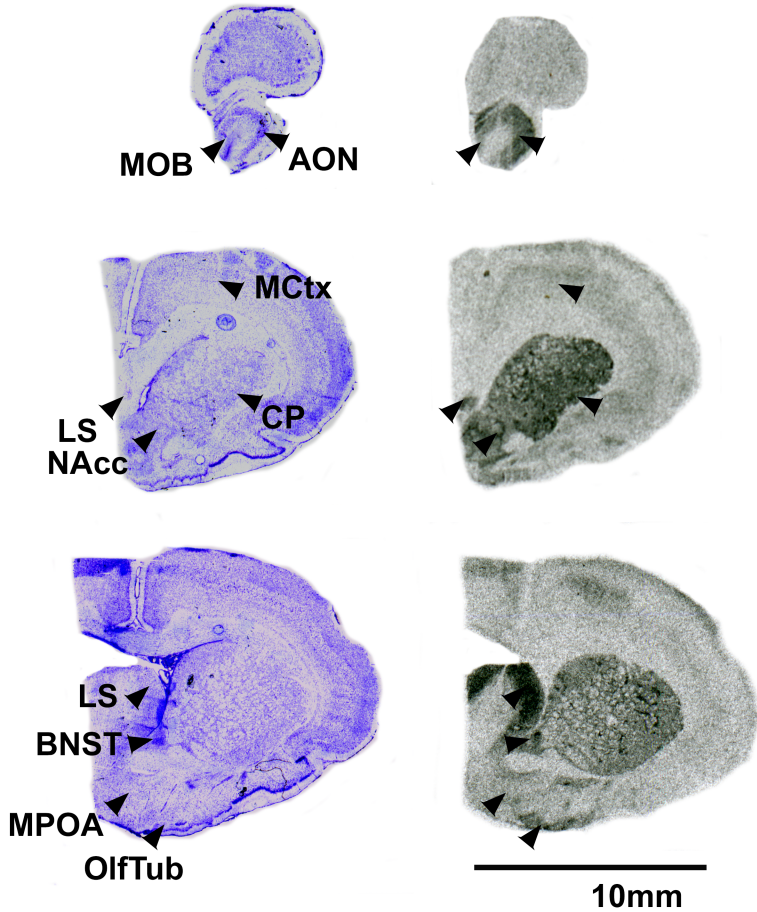


Figure 6: V1aR in the forebrain of the pouched rat. Images on left are Nissl stain, associated autoradiograms on right show V1aR density. MOB = Main olfactory bulb, AON = Accessory Olfactory Nucleus, LS = Lateral Septum, NAcc = Nucleus Accumbens, CP = Caudate Putamen, BNST = Bed Nucleus of the Stria Terminalis, MCtx = Motor Cortex, MPOA = Medial Preoptic Area, OlfTub = Olfactory Tuber.

Table 4: V1aR relative densities in select regions

Region	Relative.Binding
Olfactory Bulb	++
Nucleus Accumbens	++
mPFC	+
Ventral Pallidum	+
Lateral Septum	+++
BST	++
CeA	++
MeA	+
PVN	+

Region	Relative.Binding
Hippocampus	-
Dentate Gyrus	+
Premammillary Nucleus	++
VMH	+
VTA	+

Table 5: V1aR Maximized species Permutational Manova by family

	Df	SS	MS	F	R <sup>2</sup>	p
Family pg	5	0.4106237	0.0821247	1.464944	0.3603847	0.1548452
Residuals	13	0.7287799	0.0560600	NA	0.6396153	NA
Total	18	1.1394035	NA	NA	1.0000000	NA

Table 6: V1aR Maximized species Permutational Manova by genus

	Df	SS	MS	F	R <sup>2</sup>	p
my genus	11	0.9294802	0.0844982	2.817636	0.8157604	0.004995
Residuals	7	0.2099233	0.0299890	NA	0.1842396	NA
Total	18	1.1394035	NA	NA	1.0000000	NA

Comparing the overall patterns of binding of OTR to other rodents, the pouched rat was most similar in OTR binding to Microtus voles due to low binding in the hippocampus, but relatively high binding in the VMH (Figure 11). In these PCA biplots, the relative location of a species represents its pattern of binding in the regions identified at the end of the vectors. Therefore, species with similar receptor binding patterns will be positioned close together in the plot. The direction of these brain region vectors (i.e. arrows) indicates relative loading on PC1 and PC2, and the length of the vector indicates the weight associated with the two principal components. Therefore, a species placed near the end of a vector typically indicates relatively dense binding in that region compared to other regions in the plot.

When the number of species included in the analysis was maximized, the pouched rat was placed relatively centrally in the plot, and clustered with a number of other rodents, suggesting that the overall patterns of OTR binding in the pouched rat brain in these regions were very similar to a most other studied rodents (Figure 12).

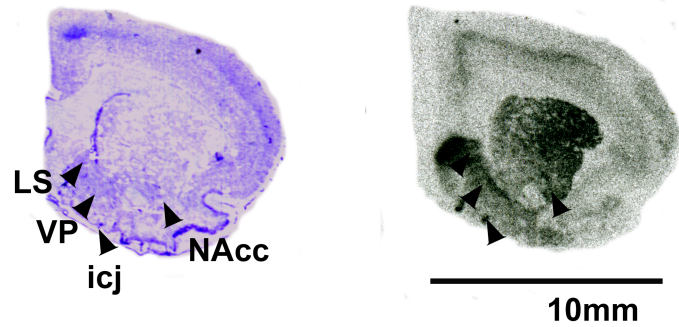


Figure 7: V1aR in the forebrain of the pouched rat. Image on left is Nissl stain, associated autoradiogram on right shows V1aR density. LS = Lateral Septum, NAcc = Nucleus Accumbens, VP = Ventral Pallidum, icj = Islands of Calleja.

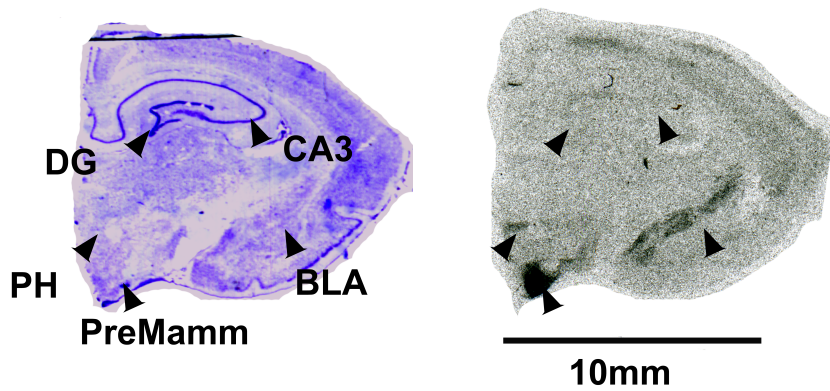


Figure 8: V1aR in the forebrain of the pouched rat. Image on left are Nissl stain, associated autoradiogram on right shows V1aR density. DG = Dentate Gyrus, CA3 = CA3 Region of the Hippocampus, BLA = Basolateral Amygdala, PH = Posterior Hypothalamus, PreMamm = Premammillary Nucleus.

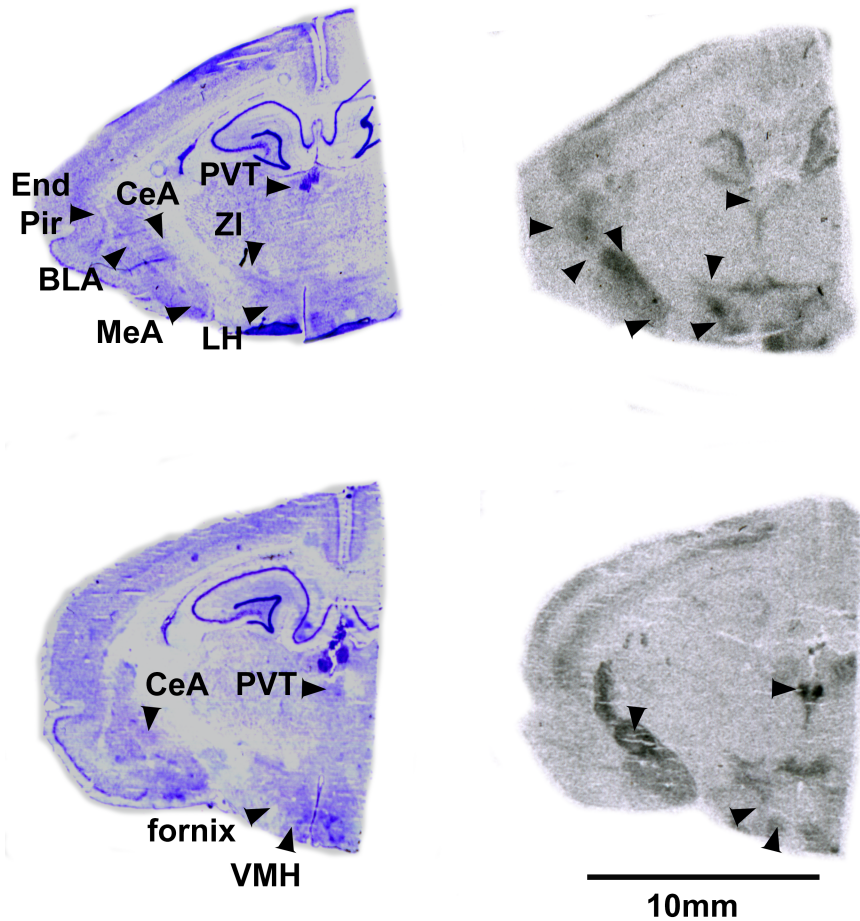


Figure 9: V1aR in the forebrain of the pouched rat. Image on left are Nissl stain, associated autoradiogram on right shows V1aR density. End Pir = Endopiriform Nucleus, BLA = Basolateral Amygdala, MeA = Medial Amygdala, CeA = Central Amygdala, VMH = Ventromedial Hypothalamic Nucleus, ZI = Zona Incerta, PVT = Periventricular Thalamic Nucleus, LH = Lateral Hypothalamus.

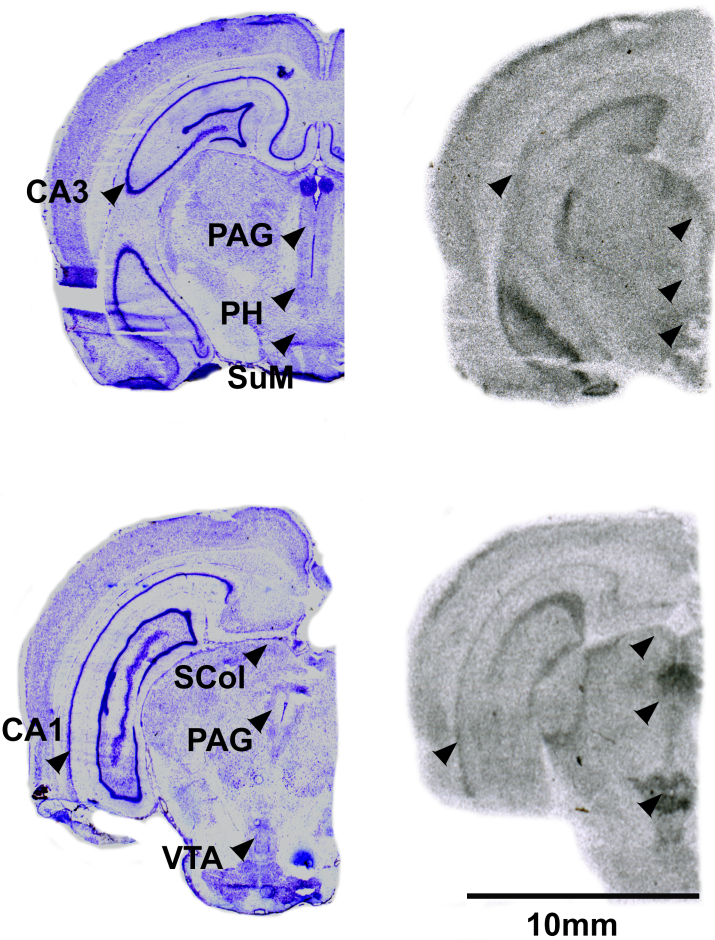


Figure 10: V1aR in the forebrain of the pouched rat. Image on left are Nissl stain, associated autoradiogram on right shows V1aR density. CA3 = CA3 region of the Hippocampus, CA1 = CA1 region of the Hippocampus, PAG = Periacqueductal Grey, PH = Posterior Hypothalamic Nucleus, SCol = Superior Colliculus, SuM = Supramammillary Nucleus, VTA = Ventral Tegmental Area.

a	Cavia	a	Heterocephalus	a	Mus	a	Rattus
a	Cricetomys	a	Meriones	a	Octodon	a	Scotinomys
a	Ctenomys	a	Microtus	a	Otomys	a	Urocitellus

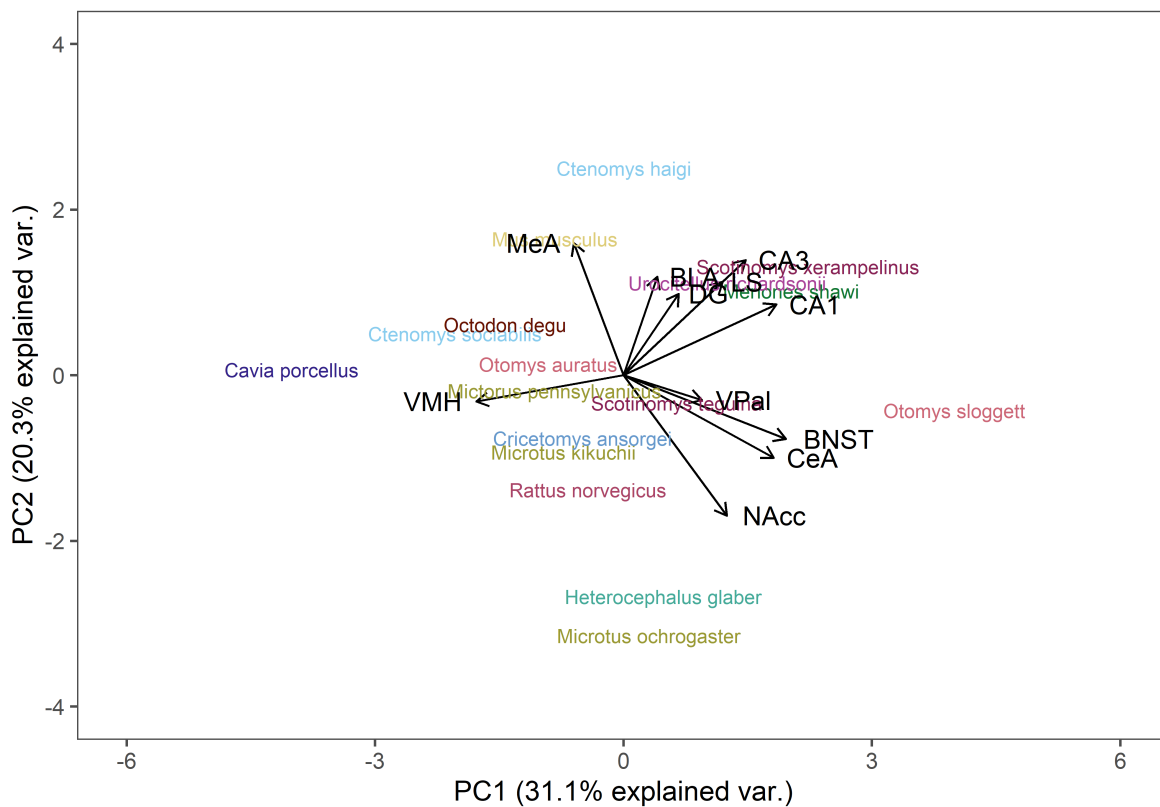


Figure 11: a PCA, OTR with regions maximized

148 The multivariate comparison of V1aR binding, with the number of species included maximized, showed that  
 149 the pouched rat was placed relatively close to the hamsters (*Phodopus sungorus*, *Meriones shawi* and *Meriones*  
 150 *unguiculatus*). However, when the number of regions included was increased, the pouched rat became more distant  
 151 from these hamsters, indicating that binding patterns in these newly included regions (the Hippocampal regions and  
 152 Basolateral amygdala) were different between hamsters and the pouched rat and resulted in additional variance. In  
 153 this analysis, with the number of regions included maximized, the pouched rat is placed between the peromyscus  
 154 mice and the microtus voles in the plot.

a	Cavia	a	Georychus	a	Mesocricetus	a	Octodon	a	Rattus
a	Cricetomys	a	Heterocephalus	a	Microtus	a	Otomys	a	Scotinomys
a	Ctenomys	a	Meriones	a	Mus	a	Peromyscus	a	Urocitellus

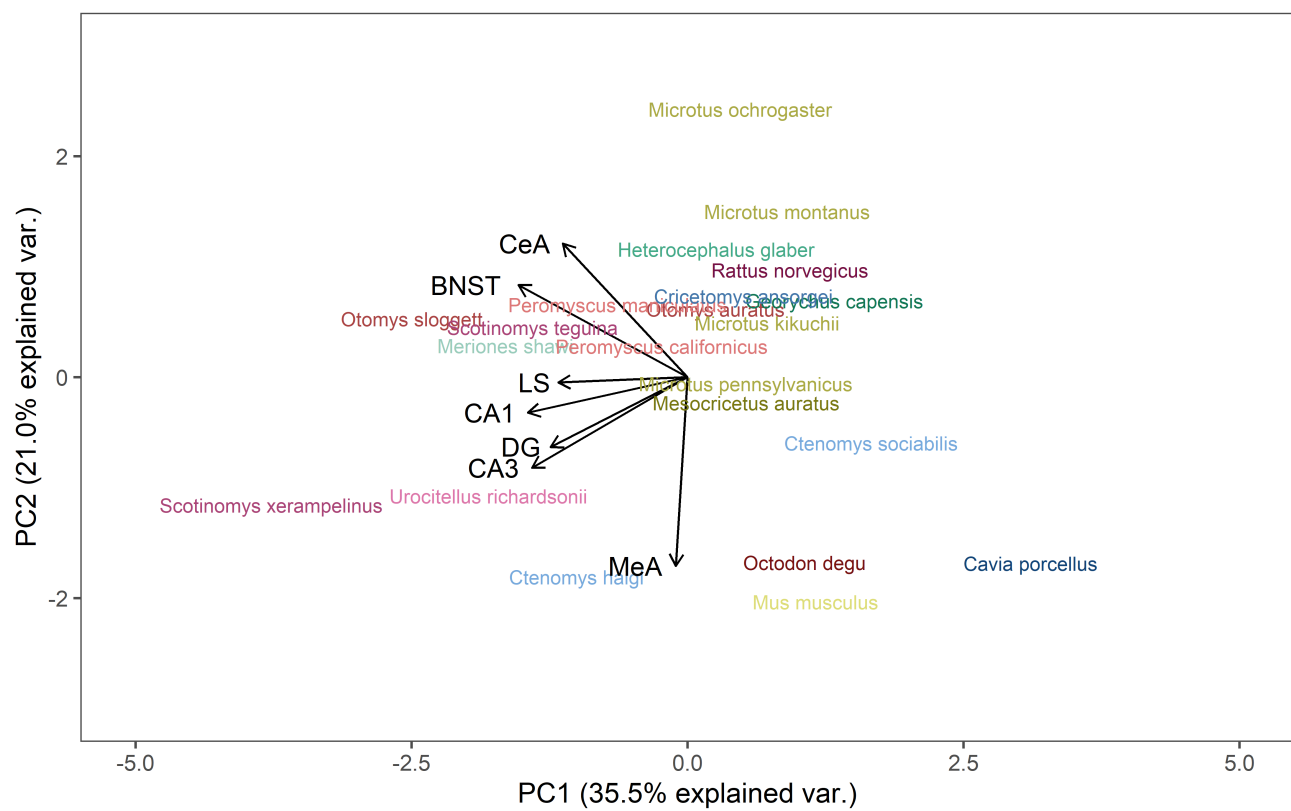


Figure 12: a PCA, OTR with species maximized

a	Cricetomys	a	Meriones	a	Mus	a	Rattus
a	Ctenomys	a	Mesocricetus	a	Peromyscus	a	Scotinomys
a	Jaculus	a	Microtus	a	Phodopus	a	Urocitellus

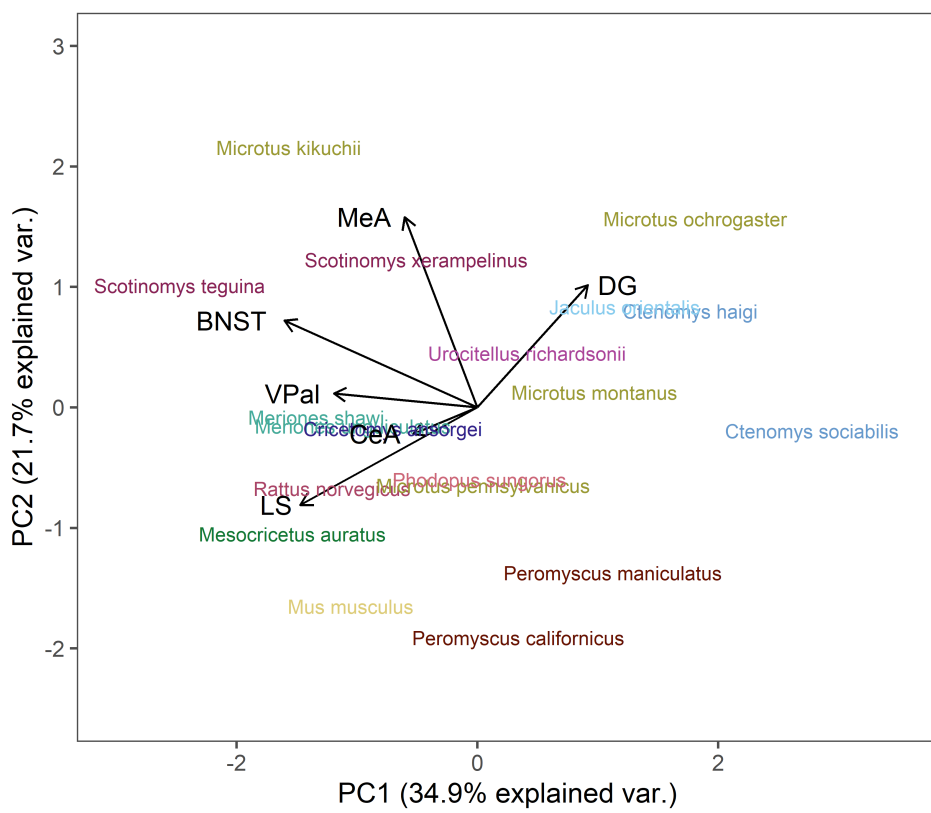


Figure 13: a PCA, V1aR with species maximized

a Cricetomys	a Meriones	a Mus	a Phodopus	a Scotinomys
a Jaculus	a Microtus	a Peromyscus	a Rattus	a Urocitellus

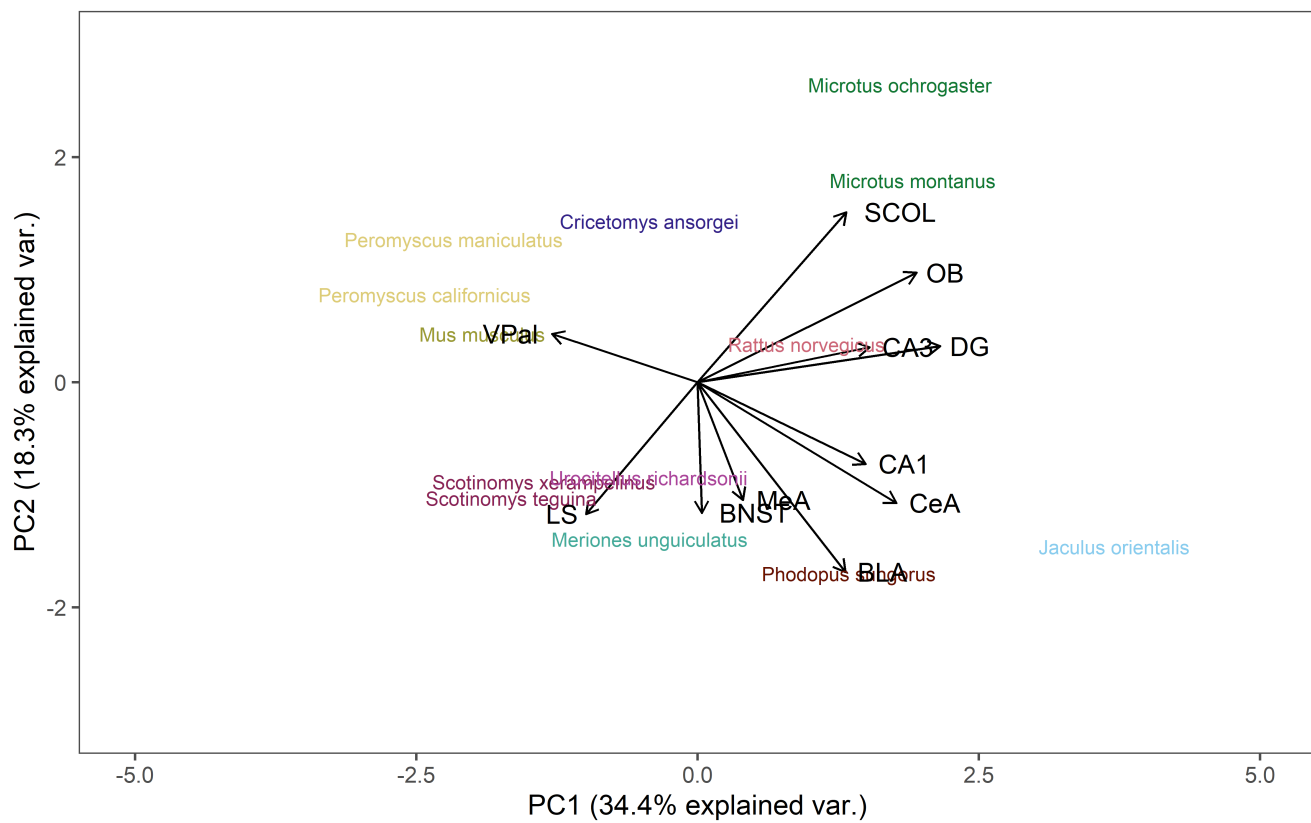


Figure 14: a PCA, V1aR with regions maximized

155 **Discussion**

- 156 -We found OTR in ... V1aR in....
- 157 -Sex differences in densities/presence and absence
- 158 -We found that overall patterns were similar to.....
- 159 -Caveats
- 160 -Unknown age
- 161 -Unknown reproductive status
- 162 -Different experiences possible
- 163 -What this means, similarities to other species
- 164 -Relevance for behavior or life history
- 165 What still needs to be known?

166 **References**

- 167 Barrett, C.E., Keebaugh, A.C., Ahern, T.H., Bass, C.E., Terwilliger, E.F., Young, L.J., 2013. Variation in vaso-  
168 pressin receptor (Avpr1a) expression creates diversity in behaviors related to monogamy in prairie voles. Hormones  
169 and behavior.
- 170 Beery, A.K., Lacey, E.A., Francis, D.D., 2008. Oxytocin and vasopressin receptor distributions in a solitary and  
171 a social species of tuco-tuco (*Ctenomys Haigi* and *Ctenomys Sociabilis*). Journal of Comparative Neurology 507,  
172 1847–1859. doi:10.1002/cne.21638
- 173 Caldwell, H.K., Albers, H.E., 2015. Oxytocin, vasopressin, and the motivational forces that drive social behav-  
174 iors, in: Behavioral Neuroscience of Motivation. Springer, pp. 51–103. doi:10.1007/7854
- 175 Campbell, P., Ophir, A.G., Phelps, S.M., 2009. Central vasopressin and oxytocin receptor distributions in two  
176 species of singing mice. Journal of Comparative Neurology 516, 321–333. doi:10.1002/cne.22116
- 177 Donaldson, Z.R., Young, L.J., 2008. Oxytocin, vasopressin, and the neurogenetics of sociality. Science 322,  
178 900–904. doi:10.1126/science.1158668 [doi]
- 179 Dubois-Dauphin, M., Theler, J.-M., Zaganidis, N., Dominik, W., Tribollet, E., Pevet, P., Charpak, G., Dreifuss,  
180 J.J., 1991. Expression of vasopressin receptors in hamster hypothalamus is sexually dimorphic and dependent upon  
181 photoperiod. Proceedings of the National Academy of Sciences of the United States of America 88, 11163–11167.

- 182 Dumais, K.M., Bredewold, R., Mayer, T.E., Veenema, A.H., 2013. Sex differences in oxytocin receptor binding in  
183 forebrain regions: Correlations with social interest in brain region- and sex- specific ways. *Hormones and Behavior*  
184 64, 693–701. doi:10.1016/j.yhbeh.2013.08.012
- 185 Dumais, K.M., Veenema, A.H., 2016. Vasopressin and oxytocin receptor systems in the brain: Sex differences and  
186 sex-specific regulation of social behavior. *Frontiers in neuroendocrinology* 40, 1–23. doi:10.1016/j.yfrne.2015.04.003
- 187 Freeman, A.R., Aulino, E.A., Caldwell, H.K., Ophir, A.G., 2020. Comparison of the distribution of oxytocin  
188 and vasopressin 1a receptors in rodents reveals conserved and derived patterns of nonapeptide evolution. *Journal*  
189 *of Neuroendocrinology* 32, e12828. doi:10.1111/jne.12828
- 190 Freeman, A.R., Hare, J.F., Caldwell, H.K., 2019. Central distribution of oxytocin and vasopressin 1a receptors  
191 in juvenile Richardson's ground squirrels. *Journal of Neuroscience Research* 97. doi:10.1002/jnr.24400
- 192 Insel, T.R., Gelhard, R., Shapiro, L.E., 1991. The comparative distribution of forebrain receptors for neu-  
193 rohypophyseal peptides in monogamous and polygamous mice. *Neuroscience* 43, 623–630. doi:10.1016/0306-  
194 4522(91)90321-E
- 195 Insel, T.R., Wang, Z., Ferris, C.F., 1994. Patterns of brain vasopressin receptor distribution associated with  
196 social organization in microtine rodents. *The Journal of Neuroscience* 14, 5381–5392. doi:10.1523/JNEUROSCI.14-  
197 09-05381.1994
- 198 Kalamantios, T., Faulkes, C.G., Oosthuizen, M.K., Poorun, R., Bennett, N.C., Coen, C.W., 2010. Telencephalic  
199 binding sites for oxytocin and social organization: A comparative study of eusocial naked mole-rats and solitary  
200 cape mole-rats. *Journal of Comparative Neurology* 518, 1792–1813. doi:10.1002/cne.22302
- 201 Kelly, A.M., Ophir, A.G., 2015. Compared to what: What can we say about nonapeptide function and social be-  
202 havior without a frame of reference? *Current opinion in behavioral sciences* 6, 97–103. doi:10.1016/j.cobeha.2015.10.010
- 203 Lim, M.M., Murphy, A.Z., Young, L.J., 2004. Ventral striatopallidal oxytocin and vasopressin V1a recep-  
204 tors in the monogamous prairie vole (*Microtus ochrogaster*). *Journal of Comparative Neurology* 468, 555–570.  
205 doi:10.1002/cne.10973
- 206 Olazábal, D.E., Sandberg, N.Y., 2020. Variation in the density of oxytocin receptors in the brain as mecha-  
207 nism of adaptation to specific social and reproductive strategies. *General and Comparative Endocrinology* 286.  
208 doi:10.1016/j.ygcn.2019.113337
- 209 Ophir, A.G., Gessel, A., Zheng, D.J., Phelps, S.M., 2012. Oxytocin receptor density is associated with male  
210 mating tactics and social monogamy. *Hormones and Behavior* 61, 445–453. doi:10.1016/j.yhbeh.2012.01.007
- 211 Ophir, A.G., Sorochman, G., Evans, B.L., Prounis, G.S., 2013. Stability and dynamics of forebrain V1aR and  
212 OTR during pregnancy in prairie voles. *Journal of neuroendocrinology* 25, 719–728. doi:10.1111/jne.12049
- 213 Ophir, A.G., Wolff, J.O., Phelps, S.M., 2008. Variation in neural V1aR predicts sexual fidelity and space use  
214 among male prairie voles in semi-natural settings. *Proceedings of the National Academy of Sciences of the United*  
215 *States of America* 105, pp. 1249–1254. doi:10.1073/pnas.0709116105

- 216 R Development Core Team, 2016. R: A language and environment for statistical computing. R Foundation  
217 for Statistical Computing, Vienna, Austria. <http://www.R-project.org/>. R Foundation for Statistical Computing,  
218 Vienna, Austria. doi:10.1007/978-3-540-74686-7
- 219 Smeltzer, M.D., Curtis, J.T., Aragona, B.J., Wang, Z., 2006. Dopamine, oxytocin, and vasopressin receptor  
220 binding in the medial prefrontal cortex of monogamous and promiscuous voles. Neuroscience letters 394, 146–151.  
221 doi:10.1016/J.NEULET.2005.10.019
- 222 Smith, C.J.W., Poehlmann, M.L., Ratnaseelan, A.M., Bredewold, R., Veenema, A.H., 2017. Age and sex  
223 differences in oxytocin and vasopressin V1a receptor binding densities in the rat brain: Focus on the social decision-  
224 making network. Brain Structure and Function 222, 981–1006. doi:10.1007/s00429-016-1260-7
- 225 Zheng, D.-J., Larsson, B., Phelps, S.M., Ophir, A.G., 2013. Female alternative mating tactics, reproductive  
226 success and nonapeptide receptor expression in the social decision-making network. Behavioural Brain Research  
227 246, 139–147. doi:10.1016/j.bbr.2013.02.024